Placenta 77 (2019) 39–45

Contents lists available at ScienceDirect

Placenta

journal homepage: www.elsevier.com/locate/placenta

Non-invasive assessment of placental perfusion in vivo using arterial spin labeling (ASL) MRI: A preclinical study in rats

Benjamin Deloison[a,b,c,d,*], Laurent J. Salomon[a,b,c,d], Thibaud Quibel[a,e], Gihad E. Chalouhi[a,b,c,d], Marianne Alison[a,f], Daniel Balvay[a], Gwennhael Autret[a], Charles-André Cuenod[a,g], Olivier Clement[a,g], Nathalie Siauve[a,c,d,g,h]

[a] INSERM, U970, Sorbonne Paris Cite, Paris Cardiovascular Research Center – PARCC, Paris, France
[b] Assistance Publique-Hôpitaux de Paris, Hôpital Necker-Enfants Malades, Paris, France
[c] EA 7328 FETUS, Université Paris Descartes, France
[d] Lumiere Project, France
[e] Department of Obstetrics and Gynecology, Poissy-Saint Germain Hospital, Versailles-Saint Quentin University, France
[f] Assistance Publique-Hôpitaux de Paris, Hôpital Robert Debré, Paris, France
[g] Assistance Publique-Hôpitaux de Paris, Hôpital Européen Georges Pompidou, Paris, France
[h] Assistance Publique-Hôpitaux de Paris, Hôpital Louis Mourier, Paris, France

ARTICLE INFO

Keywords:
Functional MRI
Placenta
Arterial spin labeling
Perfusion
Microcirculation

ABSTRACT

Introduction: Non-invasive assessment of placental perfusion is of great interest to characterize placental function in clinical practice. This article proposes a strictly non-invasive MRI technique using ASL to quantify placental blood flow in vivo. The aim of this study was to develop a fMRI tool to quantify placental blood flow (PBF) in rat, by using arterial spin labeling (ASL) MRI at 4.7 T.

Materials and methods: MRI was performed with a dedicated magnet for small animals, in pregnant rats on day 20 of the 22-day gestation period. A Look-Locker flow-sensitive alternating inversion recovery gradient echo sequence was developed as ASL technique (TE: 1.55 ms; TR: 3.5 ms, TI: 56 ms, deltaTI: 56 ms, FA: 20°, Matrix: 128 × 128, 8 segments, 4 Nex). Labeling was performed with global and slice-selective inversions, and T1 map was obtained for each mode of inversion. PBF was then derived from a compartmental model of the variation of T1 between global and slice-selective inversions.

Results: The full protocol was completed and ASL image post-processing was successful in 18 rats. Forty-seven placentas were analyzed, with a mean PBF of 147 ± 70 ml/min/100 g of placenta, consistent with published values of placental perfusion using invasive techniques.

Conclusion: ASL MRI is feasible for the quantification of PBF in rats at 4.7 T. This technique, which requires no administration of contrast media, could have implications for non-invasive longitudinal and in vivo animal studies and may be useful for the management of human pregnancies.

1. Introduction

Follow-up of pregnancy requires a growing number of imaging examinations and should benefit in the near future from advances in functional imaging. Nowadays, the initial goal of these imaging examinations is to obtain morphological data to ensure normal growth and development of the fetus and placenta, mainly by ultrasound. The current trend is to add functional data on ultrasound by using Doppler ultrasonography and 3D Doppler [1–3]. However, ultrasound and Doppler remain restricted to explore in vivo placental function including placental perfusion.

Morphologic MRI is also increasingly used as a diagnostic tool in human pregnancy to improve our diagnostic capabilities in placental or fetal pathologies [4]. Functional MRI is a booming MRI technique during pregnancy [4]. It offers various quantitative tools to better understand physiology and physiopathology and to provide important information about placental function [5–9]. Dynamic Contrast Enhancement (DCE) MRI approach can study tissue perfusion, it has been applied to murine and rat models to study placental perfusion [10–13]. However, only one placental DCE-MRI studies in humans (without quantitative parameters) [14] has been published, since it is necessary to use gadolinium chelate, which is not recommended during

* Corresponding author. INSERM, U970, Sorbonne Paris Cite, Paris Cardiovascular Research Center – PARCC, 56, rue Leblanc, Paris, France.
E-mail address: benjamin.deloison@aphp.fr (B. Deloison).

https://doi.org/10.1016/j.placenta.2019.01.019
Received 5 April 2018; Received in revised form 13 January 2019; Accepted 21 January 2019

pregnancy but may be used when the benefits outweigh the potential risks. Diffusion Weighted (DW) MRI with intravoxel incoherent motion (IVIM) provides data characterizing diffusion (ADC) and blood flow (f) of the placenta [5,15–21], however the interpretation of these parameters is still difficult [22]. Blood oxygen level–dependent (BOLD) MRI and Oxygen-Enhanced MRI can assess tissue oxygenation [23,24].

At last, Arterial spin labeling (ASL) MRI permits to measure placental perfusion [4,6,7,18,25,26]. ASL MRI technique involves the manipulation of the magnetization of arterial blood of the studied organ. This magnetically marked arterial blood is used as an endogenous tracer. It induces modifications of signal intensity (SI) in the studied organ, which are related to the perfusion. This approach, therefore, circumvents the need of intravenous injection of contrast media. Many human applications of ASL have been described, mostly for the brain, for example in strokes [27], complicated migraine [28], focal seizure [29], and in children [30].

The objective of our study, carried out at 4.7 T, is to explore the abilities of ASL for placental study and to develop an MRI approach, based on ASL, for measuring quantitatively the placental perfusion in rat and then to be able to ultimately transpose the method to pregnant women.

2. Materials and methods

2.1. Animal model

All experiments were carried out in accordance with local laws and US National Institutes of Health guidelines for animal care.

The animal model consisted in pregnant Sprague-Dawley rats (Janvier Laboratories, Le Genest St Isle, France). All MRI studies were performed on day 20.5 of the 22-day gestation period. Animals were housed under a 12 h light/12 h dark cycle, with free access to water and a standard diet. Eighteen pregnant rats were included based on previous studies of placental perfusion [12,31,32]. A schematic diagram of the rat uterus and its blood vessels is shown in Fig. 1 [33]. Two major differences between the rat uterus and the human uterus must be highlighted. The uterus of the rat is bicornuate, i.e. it is composed of two separated uterine horns, whereas the human uterus is a simplex uterus. Each horn of the rat's uterus contains several (4–8) fetoplacental units (FPU), i.e. four to eight placentas and fetuses whereas in human there is usually (with the exception of multiple pregnancies) only one placenta and one fetus.

Moreover, each horn of the rat uterus is vascularized by a uterine vascular pedicle, the main source of blood which arises from the homolateral iliac artery, and an ovarian vascular pedicle which arises from the abdominal *aorta.*. The uterine and ovarian arteries form an arch on the inner side of the uterine horns. Superior blood supply to uterine horns originates from the a aorta, whereas inferior blood supply originates from the common iliac artery.

At the level of the placenta, the blood (coming from the arch) flows through a central vessel perpendicular to the great transverse axis of the placenta, and then the blood is distributed from the chorionic plate to vascular lakes with multidirectional flows in the intervillous chamber.

2.2. Animal preparation for MRI

Anesthesia was induced with 5% isoflurane (Baxter, Maurepas, France) in oxygen (1 l/min) and maintained with about 1.5% isoflurane supplied through a nose cone during MRI. Anesthesia was monitored regularly throughout the procedure. Temperature was monitored and maintained at 37 °C with a controlled-temperature heating pad. Respiration was also monitored with custom-made hardware and software (SA Instruments Inc., Stony Brook, NY, USA).

After MRI, the mother and her litter were euthanized, under anesthesia, by intravenous pentobarbital injection (150 mg/kg).

2.3. Imaging protocol

MRI was performed with a small animal-dedicated MRI scanner (Biospec 47/40 USR, Bruker Biospin, Ettlingen, Germany) with a magnetic field of 4.7 T. Anesthetized animals were placed in the supine position in a rat-dedicated quadrature transmit/receive body coil with an internal diameter of 7 cm. MRI was carried out after standard spectrometer adjustments (coil tuning/matching, RF gain calibration).

Anatomic images with a high-resolution scan were acquired before the ASL sequence.

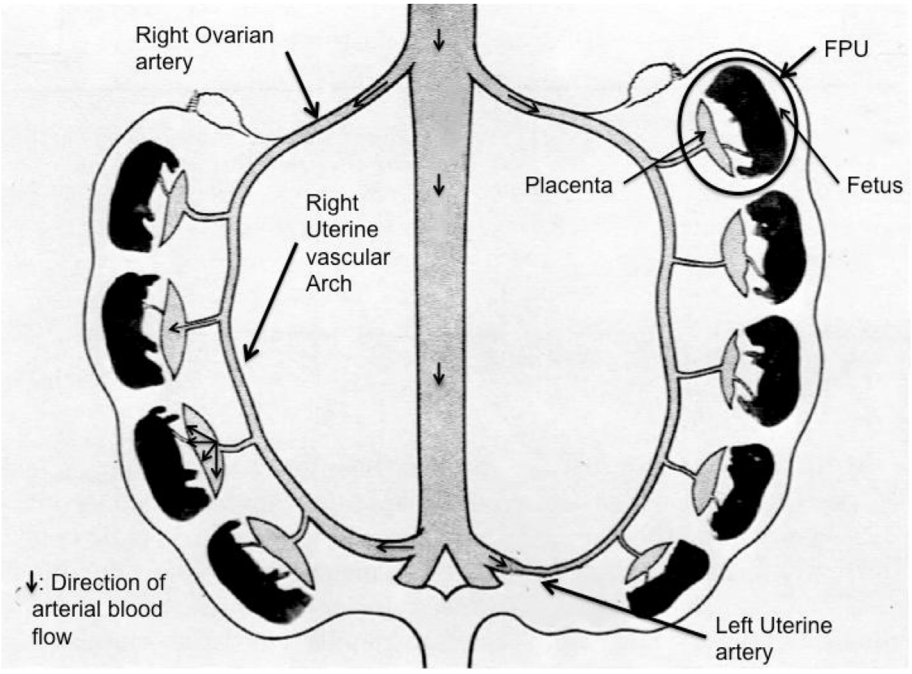

Fig. 1. Schematic diagram of rat's uterus and placenta vascularization, adapted from Wigglesworths [27]. (FPU: Feto-Placental Unit)`.

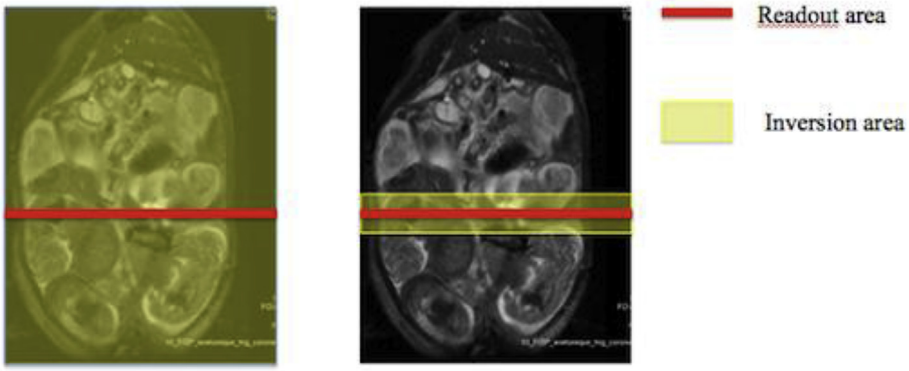

Fig. 2. Schematization of the flow-sensitive alternating inversion recovery sequence used for the placenta with selective and global inversion (in yellow) and the readout area (in red), corresponding to acquired images.

2.3.1. Anatomic sequence

A two-dimensional fast imaging with steady state precession sequence in the three spatial planes (20 slices each) was used to identify the FPUs and their location within the horns. The parameters of this sequence were: TR 3.2 ms, TE 1.6 ms, FA: 60°, FOV 7 × 7 cm, BW: 150 kHz, matrix 256 × 256, section thickness: 2 mm.

2.3.2. ASL sequence

A Look-Locker based ASL acquisition with longitudinal relaxation (T1) mapping already described elsewhere [34] was specifically adapted for the study of PBF. The magnetic labeling was obtained by a pulse ASL (PASL) technique, using an inversion recovery (IR) pulse. Two sets of images were obtained with two different types of magnetic labeling. For the first set of images, a global inversion pulse was applied within the whole imaged volume: every blood's protons within the sensitive volume of the transmit coil are labeled. For the second set of images, a selective inversion pulse was performed to a 2 mm-thick axial slice, chosen on the anatomic sequences to contain the largest number of placentas. During this selective inversion, only the blood's protons of the slice of interest are labeled (Fig. 2).

Since ASL is very sensitive to motion artifacts, cardiac and/or respiratory gating is often used, but to limit acquisition times and avoid the effects of prolonged anesthesia, we did not use any gating. To reduce the effect of any motion artifact, the placentas chosen for analysis were as far away as possible from the diaphragm.

The imaging sequence was a gradient echo sequence, with the following parameters: TE: 1.55 ms; TR: 3.5 ms, TI = 56 ms, FA 20°, 8 segments, 4 Nex, Matrix: 128 × 128, FOV: 7 × 7cm, i.e. pixel size was 0.54 × 0.54 mm. A single 2 mm-thick axial slice was available, which corresponded to the slice of interest of the selective labeling.

For the T1 mapping, 40 images with different times of inversion (TI) were acquired, at 56 ms (16 TR) intervals (from 78 ms to 2316 ms), for each selective and global inversion pulse. The total acquisition time of the ASL sequence was about 13 min.

2.4. Image post-processing

All images were transferred to the workstation Paravision 5 (Bruker Biospin MRI GmbH, Ettlingen, Germany) and analyzed with the available dedicated ASL software module. The series of images obtained with the global inversion was the control series and the series of images obtained with slice selective inversion was the labeled series.

2.4.1. T1 maps

The SI recovery curve as a function of TI for the whole slice was fitted by the least squares method, as follows [34] to obtain experimental values of T1 (T1app) in each sets of images (slice-selective and global IR):

$$\mathbf{S(Ti(n)} = \mathbf{S0}(1-\mathbf{2}\exp(\mathbf{Ti(n)}/\mathbf{T1p}))) \quad (1)$$

Where S (Ti(n)) is the SI of each pixel of a series of raw images, S0 is the signal corresponding to magnetization under partial saturation, Ti(n) is the TI of the nth image of the series. Ti(n) values were obtained as averages of the TIs measured over all phase-encoding steps.

A correction of the experimental values of T1 (T1app) was necessary to obtain the actual values of T1 (T1), because the magnetization was partially saturated by the excitation pulses. The T1app is indeed shorter than the actual T1, and was corrected, using the following equation [34,35]:

$$1/T1app = 1/T1 + (\log(\cos\alpha))/TR \quad (2)$$

Where α corresponding to the flip angle of the sequence.

Two T1 maps were calculated for the slice-selective and global IR experiments.

2.4.2. PBF

Kober et al. and Belle et al. developed a model describing the effect of perfusion on longitudinal relaxation time in heart [34,36]. This model was adapted to the study of placenta (annexe 1).

The difference between selective inversion and global inversion magnetization is directly related to blood flow. The PBF was then calculated from the T1 maps as follows [34,36]:

$$PBF = \lambda\ T1\ global\ [(1/T1\ sel)-(1/T1\ global)]. \quad (6)$$

Where λ is assumed to be 0.9 ml/g for the placenta [6,37], to allow the results to be expressed in familiar units.

2.4.3. Perfusion maps

The global inversion T1 map was subtracted from the selective inversion T1 map, to obtain a delta T1 map, which was converted to the perfusion map.

The placentas were recognized on the first image of the ASL sequence and on the anatomic sequence. One region of interest (ROI) for each placenta was manually delineated, covering the entire surface of each placenta. This ROI was then copied onto the parametric perfusion map, to obtain the PBF in ml/min/100 g.

The ASL parameters were expressed as means and standard deviations (SD).

3. Results

3.1. Animal model

Eighteen pregnant rats, with a mean weight of 366 g (± 33 g), were included in the study.

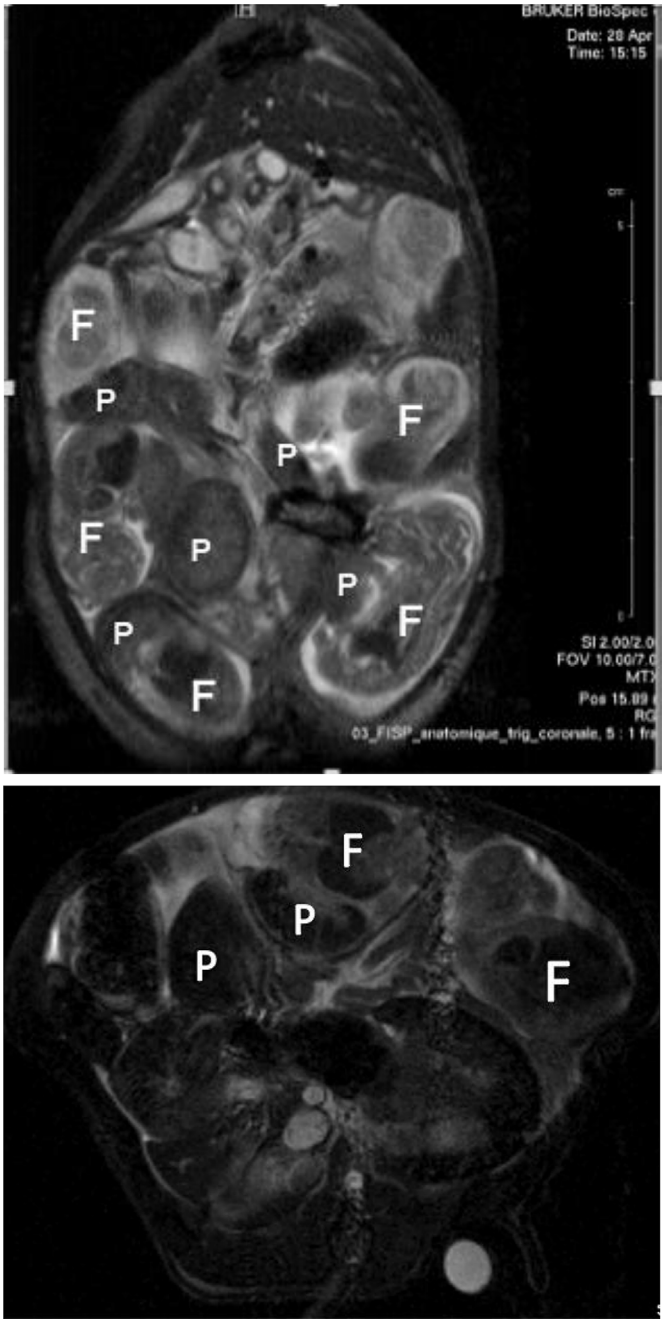

Fig. 3. Coronal and axial views of the rat abdomen in true FISP MR imaging sequences at 4.7 T showing feto-placental units with fetuses (F) and placentas (P). In the coronal view, three FPUs are located in the right horn, and two FPUs are located in the left horn. In the axial view, only one FPU is visible. One additional fetus from the left horn and one placenta from the right horn are depicted.

3.2. Imaging protocol

3.2.1. Anatomic sequence

The spatial resolution of the two-dimensional fast imaging with steady state precession sequence at 4.7 T was sufficient for the spotting of all the placentas, with a SI similar to that of muscle, and all the corresponding fetuses (Fig. 3). The number of placentas visualized per slice varied from 1 to 6. Mean placental thickness was 3.4 (± 0.7) mm.

3.2.2. ASL sequence

Each set of 40 images was obtained with the various TI in each global and selective acquisition. Fig. 4 shows 16 images of each set obtained after the slice-selective and global inversions. The SI decreases rapidly after the inversion and then gradually increases.

3.3. Image post-processing

3.3.1. Perfusion maps

An example of perfusion map is shown in Fig. 5. Placentas were delineated on anatomic image. For the 18 rats, the median and mean numbers of observable placentas on ASL MR images were 2 and 2.6, respectively (range: 1–7).

3.3.2. Placental blood flow (PBF)

Quantitative analyze of perfusion was performed in 47 placentas of the 18 rats. The ROI size was 0.51 cm^2 (± 0.17). Mean perfusion was 147 ± 70 ml/min/100 g. The quantitative PBF values are summarized in Table 1.

4. Discussion

4.1. Main findings

These results demonstrate that quantifying placental perfusion by ASL MRI is feasible in small animals, using a small dedicated MR magnet with a strong magnetic field (4.7 T). ASL allowed us to study 47 placentas from 18 rats and to measure the placental blood flow (PBF), which was equal to 147 ml/min/100 g (± 70). This parameter describes tissue perfusion in ml/min/100 g of placenta (i.e. blood circulation within the parenchyma of the organs). The values obtained compare favorably with previous evaluations of placental perfusion in animals based on DCE MRI (126–180 ml/min/100 ml) [6,11–13,38] since the density of the placenta is almost 1 g/ml [39].

These results are very inspiring and may have a tangible potential for investigation of the placenta with a quantitative estimation of placental perfusion. Indeed, the opportunity to explore the placental function through physiological data is of great interest, especially when it comes to placental blood flow. High levels of uterine vascular resistance or low levels of uterine blood flow may decrease placental perfusion, thereby causing fetal growth restriction (FGR) and vascular complications to the fetus and the mother [40–42]. However, the etiologies and pathogenesis of uteroplacental disorders are poorly documented, and placental function remains difficult to assess in routine clinical practice by ultrasound [1,2,43–45].

Assessment of PBF in animals offers new perspectives. This is a complementary approach to human studies to increase knowledge placental insufficiency. It may permit a better characterization of placental perfusion in case of genetic and developmental abnormalities, targeted defects of placental function, fetal growth restriction, preeclampsia, and fetal death in utero.

4.2. Technical considerations

ASL is based on the principle of an electromagnetic labeling of the spins of water protons in the feeding arteries before they flow into the studied tissue. We developed a pulse arterial spin labeling (PASL) technique, which is more appropriate for the study of a multidirectional flow like in a placenta and which could be more easily adapted to human pregnancies. With PASL, two states of labeling are compared. A labeling of the arterial spin is performed inside the organ in a selected slice and corresponds to the labeled experiment. A global labeling of all the arterial spins of the blood throughout the study volume corresponds to the control experiment. With this labeling obtained by a global inversion, all the protons of water are inverted to cancel out the signal from the blood throughout the study volume. MR acquisition after the labeling provides images where all the arterial spins of the blood are inverted. The PASL approach was initially proposed by Kwong et al.

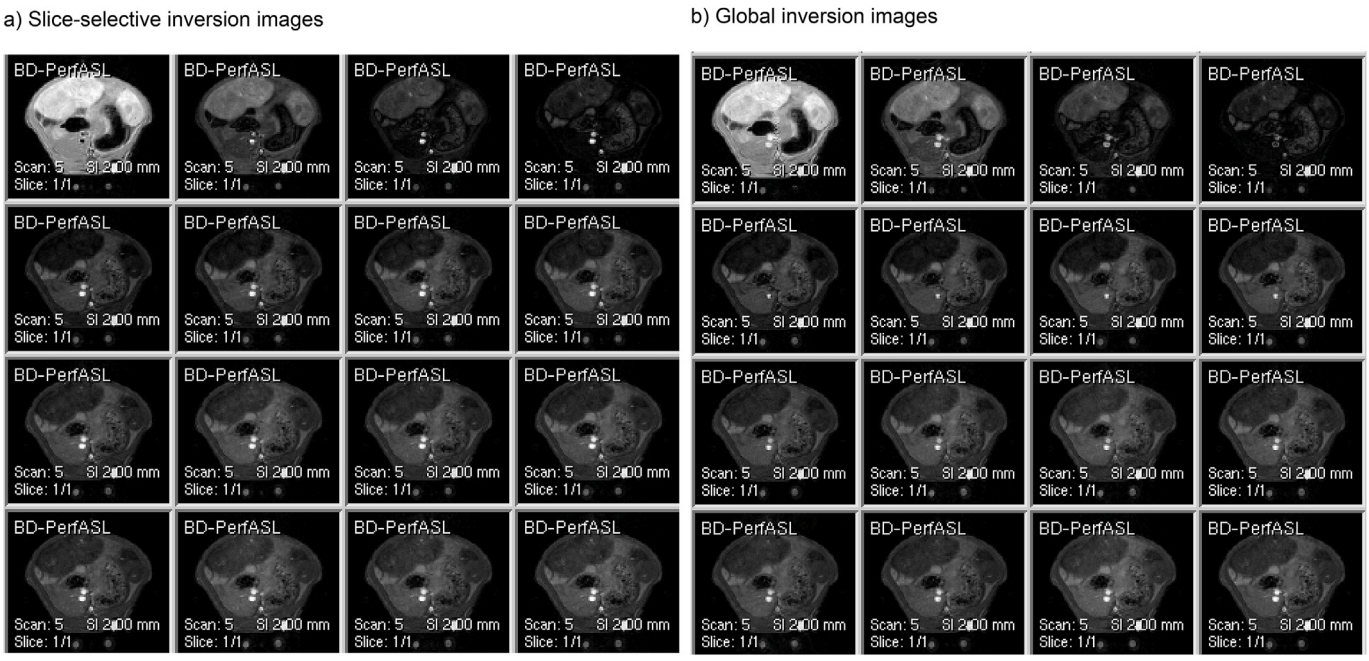

Fig. 4. Set of 16 images from the ASL series following slice-selective (**a**) and global (**b**) inversions of magnetization. The first image (at the top right) was obtained before inversion. The second image was obtained at TI = 78 ms and has the highest SI. For the 14 remaining images, the TI varied from 134 ms to 862 ms, i.e. with a 56 ms increase for each image. SI rapidly decreased after inversion, until the fifth image, gradually increasing thereafter. This pattern of behavior was observed for both selective and global inversions.

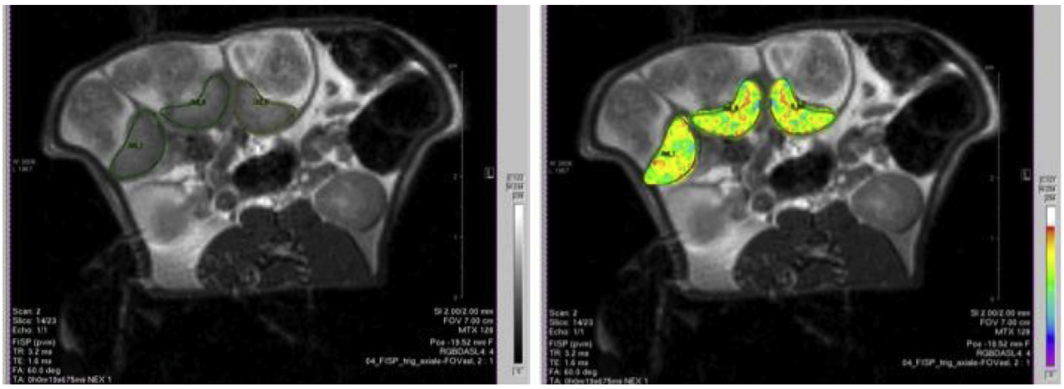

Fig. 5. Perfusion map for a pregnant rat, in axial view. The first image is the anatomic true FISP image in axial view and the second is the fusion of the perfusion map on the anatomical image. The placentas were located on the anatomical image and ROI were drawn and projected onto the perfusion map to obtain the perfusion values for the ROI.

Table 1
Mean perfusion values for all placentas.

	Number of placentas	Perfusion (ml/min/100 ml)	SD (ml/min/100 ml)
Right horn	28	166	88
Left horn	19	124	55
Total	47	147	70

$p = 0.13$ for the difference between the right and left horns.

[46] and reported by Kim [47] and Schwarzbauer et al. [48] for the quantification of cerebral blood flow. Gowland et al. [6] also used it for placental study but at 0.5 T.

4.3. Quantification of placental blood flow

The quantification of the placental blood flow is based on the values of the longitudinal relaxation time T1, which is calculated pixel by pixel and represented on map. A flow-sensitive alternating inversion recovery sequence with multiple time of inversion (TI) was used to obtain T1 maps: the T1 map of the global inversion and the T1 map of the selective inversion. These T1 maps allowed quantifying placental perfusion from the global T1 and from the subtraction between $1/T1_{selective}$ and $1/T1_{global}$. We then obtain a PBF mapping pixel by pixel and therefore an average value of the perfusion from a ROI.

4.4. Placental model

In rats, vascularization of the uterine horn is through an archway to its inside, fed by ovarian artery (which arises from the abdominal aorta) and uterine artery (which arises from the iliac artery). This vascular arch gives the placental arterial input and the flow direction is perpendicular to the arcade and is made in a transverse axial plane. The placental blood flows are multidirectional: blood enters the placenta via a central vessel perpendicular to the great transverse axis of the placenta, and then it is distributed from the chorionic plate to vascular

lakes with multidirectional flows in the intervillous chamber. Our dedicated placental ASL studies PBF in the intervillous chamber, which corresponds to the overall placental perfusion across the voxel.

4.4.1. Advantages of ASL MRI

ASL has many advantages for the study of placental perfusion during pregnancy compared to other functional MRI techniques. ASL is the only fMRI technique that gives a quantitative measurement of placental blood flow without any invasiveness. DCE MRI is the other concurrent method but it requires the use of an intravascular injection of contrast agent. Others fMRI techniques without any invasiveness are also available. DW MRI with (IVIM) [32] is an interesting approach, and has been already used to describe the placenta [5,15–21] with the perfusion fraction (f), expressed in % and the pseudo diffusion coefficient D* expressed in mm^2/s. The physiological relevance of these parameters is not yet clear [22]. At last, BOLD MRI and OE MRI study tissue oxygenation [23,24] and appear to be complementary to the study of the blood flow.

ASL approach may have a tangible potential for investigation of the placenta in humans with a quantitative estimation of placental perfusion. In 1998, Francis et al. [7] and Gowland et al. [6] used ASL at 0.5 T in pregnant women and obtained a value for PBF of 176 ml/min/100 g (± 91 ml/min/100 g), which is also similar our results. In 2013 Derwig [6,18] used ASL in the second trimester of pregnancy and concluded that placental perfusion could be a strong indicator of future gestational outcome.

4.5. Limitations

Compared to other fMRI techniques, ASL suffers from a low sensitivity due to poor signal-to-noise ratio (SNR) and susceptibility to motion artifacts. The SNR can be improved by increasing the magnetic field. A small dedicated MR magnet with a strong magnetic field (4.7 T) was used in this study. Nevertheless, the SNR obtained was low, only few %. In human, the use of a 3T would improve the SNR, however, there is little data regarding the use of high magnetic fields during pregnancy.

Vascular artifacts may be present, in the form of high signal intensity in vascular structures, when labeled protons remain in vessels. This phenomenon exists when the time it takes for the blood to move from the labeled slice to the slice of interest, i.e. blood transit time, is too long compared to the acquisition time. These vascular artifacts can lead to overestimating the perfusion. No data exists in the literature about placental blood transit time.

The use of a λ (tissue-to-blood partitioning coefficient) of 0.9 [6,37] and a $T1_{blood}$ of 1600 ms [34] was based on other literature studies, but these two values are unknown and this could also be a limitation of our study. This choice may have affected the results by causing a possible systematic error of the absolute value of PBF but does not affect its relative value and the variability of the results.

Some other technical issues related to small animal use must be considered. We were forced to use a single slice sequence to reduce the time of acquisition. It is a limitation of our study because only a part of the volume of the placenta is assessed, and the slice may contain amniotic fluid or another structural feature. However, mean placental thickness in rat is 3.4 mm, and the slices used in the sequence were 2 mm thick. We therefore considered that the PBF obtained provides a good indication of mean placental perfusion, particularly as the results obtained were consistent with those of other studies. In human studies, multi-slices should be used and an analysis of the entire placental volume will be necessary.

At last, ASL is very sensitive to motion artifacts, however, no cardiac or respiratory gating was used, in order to keep the acquisition times low, and avoid any effects due to prolonged anesthesia. To reduce the effect of any motion artifacts, placentas chosen for analysis were as far removed from the diaphragm as possible.

Both the lack of gating, and the single slice use contribute to the variability of our results and make it difficult to immediately adapt this technique to human. Limitations related to small animals use must be taken into account for application of ASL to humans.

5. Conclusion

ASL MRI is feasible to study the perfusion of the placenta in rats, at 4.7 T, with a quantitative physiological parameter expressed in ml/min/100 g. This fMRI method is the only one that gives a quantitative assessment of perfusion without any invasiveness, i.e. without even an IV injection of contrast media, and is particular tailored to the placental study in human.

Assessment of PBF in animals offers new perspectives to better explore placental function.

This study also addresses some of the challenges of placental ASL to adapt the technique to clinical practice and shows the potential applications for the diagnosis of placental insufficiency.

Conflicts of interest

The authors report no conflict of interest.

Annexe 1

A two-compartment model has described the effect of perfusion on longitudinal relaxation time: one compartment is the intravascular capillary blood and the other is the extravascular tissue. Both compartments are characterized by their own longitudinal nuclear magnetization M(t) governed by their intrinsic relaxation time T1, and with exchange rates of water molecules between capillary space and extravascular tissue. M(t) behaves like a biexponential function in theory.

By making the same assumption as Kober and Belle: M(t) can be approximated by M(t) exp (- t/T1), the longitudinal relaxation time T1 in placenta can be obtained from the variation of the SI in placenta, using the following equation:

$$T1 = \int_0^{|} M(t).\, dT \tag{3}$$

Solving equation (3) in both experimental conditions (selective and global inversions) and taking into account that the approximation of a fast exchange between intracapillary and extravascular space may be assumed leads to the following expressions:

$$\frac{1}{T1\ selective} = \frac{P}{\lambda} + \frac{1}{T0} \tag{4}$$

$$\frac{1}{\mathrm{T1\ global}} = \frac{\frac{1}{\mathrm{T0}} + \frac{\mathrm{P}}{\lambda}}{1 + \frac{\mathrm{P.\,T1\ blood}}{\lambda}} \tag{5}$$

where λ is the tissue-to-blood partitioning coefficient for water and P is the perfusion.

and $T1_{blood}$ was supposed to be 1600 ms [34].

References

[1] O. Morel, G. Grange, J. Fresson, J.P. Schaaps, J.M. Foidart, D. Cabrol, V. Tsatsaris, Vascularization of the placenta and the sub-placental myometrium: feasibility and reproducibility of a three-dimensional power Doppler ultrasound quantification technique. A pilot study, J. Matern. Fetal Neonatal Med. : Offic. J. Eur. Assoc. Perinat. Med., Fed Asia Oceania Perinat. Soc., Int. Soc. Perinat. Obstet. 24 (2) (2011) 284–290.

[2] J. Duan, E. Perdriolle-Galet, A.C. Chabot-Lecoanet, R. Callec, M. Beaumont, P. Chavatte-Palmer, V. Tsatsaris, O. Morel, Placental 3D Doppler angiography: current and upcoming applications, J. Gynecol. Obstet. Biol. Reprod. 44 (2) (2015) 107–118.

[3] W. Sun, J. Liu, Y. Zhang, A. Cai, Z. Yang, Y. Zhao, Y. Wang, Z. Cao, Q. Wei, Quantitative assessment of placental perfusion by three-dimensional power Doppler ultrasound for twins with selective intrauterine growth restriction in one twin, Eur. J. Obstet. Gynecol. Reprod. Biol. 226 (2018) 15–20.

[4] N. Siauve, G.E. Chalouhi, B. Deloison, M. Alison, O. Clement, Y. Ville, L.J. Salomon, Functional imaging of the human placenta with magnetic resonance, Am. J. Obstet. Gynecol. 213 (4 Suppl) (2015) S103–S114.

[5] H.M. Bonel, B. Stolz, L. Diedrichsen, K. Frei, B. Saar, B. Tutschek, L. Raio, D. Surbek, S. Srivastav, M. Nelle, J. Slotboom, R. Wiest, Diffusion-weighted MR imaging of the placenta in fetuses with placental insufficiency, Radiology 257 (3) (2010) 810–819.

[6] P.A. Gowland, S.T. Francis, K.R. Duncan, A.J. Freeman, B. Issa, R.J. Moore, R.W. Bowtell, P.N. Baker, I.R. Johnson, B.S. Worthington, In vivo perfusion measurements in the human placenta using echo planar imaging at 0.5 T, Magn. Reson. Med.: Offic. J. Soc. Magn. Reson. Med./Soc. Magn. Reson. Med. 40 (3) (1998) 467–473.

[7] S.T. Francis, K.R. Duncan, R.J. Moore, P.N. Baker, I.R. Johnson, P.A. Gowland, Non-invasive mapping of placental perfusion, Lancet 351 (9113) (1998) 1397–1399.

[8] R. Avni, T. Raz, I.E. Biton, V. Kalchenko, J.R. Garbow, M. Neeman, Unique in utero identification of fetuses in multifetal mouse pregnancies by placental bidirectional arterial spin labeling MRI, Magn. Reson. Med. : Offic. J. Soc. Magn. Reson. Med./Soc. Magn. Reson. Med. 68 (2) (2012) 560–570.

[9] R. Brunelli, G. Masselli, T. Parasassi, M. De Spirito, M. Papi, G. Perrone, E. Pittaluga, G. Gualdi, E. Pollettini, A. Pittalis, M.M. Anceschi, Intervillous circulation in intrauterine growth restriction. Correlation to fetal well being, Placenta 31 (12) (2010) 1051–1056.

[10] B. Deloison, N. Siauve, S. Aimot, D. Balvay, R. Thiam, C.A. Cuenod, Y. Ville, O. Clement, L.J. Salomon, SPIO-enhanced magnetic resonance imaging study of placental perfusion in a rat model of intrauterine growth restriction, BJOG An Int. J. Obstet. Gynaecol. 119 (5) (2012) 626–633.

[11] M. Alison, T. Quibel, D. Balvay, G. Autret, C. Bourillon, G.E. Chalouhi, B. Deloison, L.J. Salomon, C.A. Cuenod, O. Clement, N. Siauve, Measurement of placental perfusion by dynamic contrast-enhanced MRI at 4.7 T, Invest. Radiol. 48 (7) (2013) 535–542.

[12] L.J. Salomon, N. Siauve, D. Balvay, C.A. Cuenod, C. Vayssettes, A. Luciani, G. Frija, Y. Ville, O. Clement, Placental perfusion MR imaging with contrast agents in a mouse model, Radiology 235 (1) (2005) 73–80.

[13] L.J. Salomon, N. Siauve, F. Taillieu, D. Balvay, C. Vayssettes, G. Frija, Y. Ville, C.A. Cuenod, O. Clement, In vivo dynamic MRI measurement of the noradrenaline-induced reduction in placental blood flow in mice, Placenta 27 (9–10) (2006) 1007–1013.

[14] A.E. Millischer, B. Deloison, S. Silvera, Y. Ville, N. Boddaert, D. Balvay, N. Siauve, C.A. Cuenod, V. Tsatsaris, L. Sentilhes, L.J. Salomon, Dynamic contrast enhanced MRI of the placenta: a tool for prenatal diagnosis of placenta accreta? Placenta 53 (2017) 40–47.

[15] R.J. Moore, B.K. Strachan, D.J. Tyler, K.R. Duncan, P.N. Baker, B.S. Worthington, I.R. Johnson, P.A. Gowland, In utero perfusing fraction maps in normal and growth restricted pregnancy measured using IVIM echo-planar MRI, Placenta 21 (7) (2000) 726–732.

[16] S. Sohlberg, A. Mulic-Lutvica, P. Lindgren, F. Ortiz-Nieto, A.K. Wikstrom, J. Wikstrom, Placental perfusion in normal pregnancy and early and late pre-eclampsia: a magnetic resonance imaging study, Placenta 35 (3) (2014) 202–206.

[17] I. Derwig, G.J. Barker, L. Poon, F. Zelaya, P. Gowland, D.J. Lythgoe, K. Nicolaides, Association of placental T2 relaxation times and uterine artery Doppler ultrasound measures of placental blood flow, Placenta 34 (6) (2013) 474–479.

[18] I. Derwig, D.J. Lythgoe, G.J. Barker, L. Poon, P. Gowland, R. Yeung, F. Zelaya, K. Nicolaides, Association of placental perfusion, as assessed by magnetic resonance imaging and uterine artery Doppler ultrasound, and its relationship to pregnancy outcome, Placenta 34 (10) (2013) 885–891.

[19] A.K. Sivrioglu, U. Ozcan, A. Turk, S. Ulus, M.E. Yildiz, G. Sonmez, H. Mutlu, Evaluation of the placenta with relative apparent diffusion coefficient and T2 signal intensity analysis, Diagn. Interventional Radiol. 19 (6) (2013) 495–500.

[20] L. Manganaro, F. Fierro, A. Tomei, L. La Barbera, S. Savelli, P. Sollazzo, M.E. Sergi, V. Vinci, L. Ballesio, M. Marini, MRI and DWI: feasibility of DWI and ADC maps in the evaluation of placental changes during gestation, Prenat. Diagn. 30 (12–13) (2010) 1178–1184.

[21] R.J. Moore, S.S. Ong, D.J. Tyler, R. Duckett, P.N. Baker, W.R. Dunn, I.R. Johnson, P.A. Gowland, Spiral Artery Blood Volume in Normal Pregnancies and Those Compromised by Pre-eclampsia, NMR in Biomedicine, (2007).

[22] D. Le Bihan, What can we see with IVIM MRI? Neuroimage (2017 Dec 22), https://doi.org/10.1016/j.neuroimage.2017.12.062 pii: S1053-8119(17)31086-8.

[23] I. Huen, D.M. Morris, C. Wright, G.J. Parker, C.P. Sibley, E.D. Johnstone, J.H. Naish, R1 and R2 * changes in the human placenta in response to maternal oxygen challenge, Magn. Reson. Med. 70 (5) (2013) 1427–1433.

[24] A. Sorensen, D. Peters, E. Frund, G. Lingman, O. Christiansen, N. Uldbjerg, Changes in human placental oxygenation during maternal hyperoxia as estimated by BOLD MRI, Ultrasound Obstet. Gynecol.: Offic. J. Int. Soc. Ultrasound Obstet. Gynecol. (2013).

[25] X. Shao, D. Liu, T. Martin, T. Chanlaw, S.U. Devaskar, C. Janzen, A.M. Murphy, D. Margolis, K. Sung, D.J.J. Wang, Measuring human placental blood flow with multidelay 3D GRASE pseudocontinuous arterial spin labeling at 3T, J. Magn. Reson. Imag. : JMRI 47 (6) (2018) 1667–1676.

[26] Z. Zun, C. Limperopoulos, Placental perfusion imaging using velocity-selective arterial spin labeling, Magn. Reson. Med. : Offic. J. Soc. Magn. Reson. Med./Soc. Magn. Reson. Med. 80 (3) (2018) 1036–1047.

[27] J.A. Chalela, D.C. Alsop, J.B. Gonzalez-Atavales, J.A. Maldjian, S.E. Kasner, J.A. Detre, Magnetic resonance perfusion imaging in acute ischemic stroke using continuous arterial spin labeling, Stroke; A J. Cereb. Circ. 31 (3) (2000) 680–687.

[28] J.M. Pollock, A.R. Deibler, J.H. Burdette, R.A. Kraft, H. Tan, A.B. Evans, J.A. Maldjian, Migraine associated cerebral hyperperfusion with arterial spin-labeled MR imaging, AJNR. Am. J. Neuroradiol. 29 (8) (2008) 1494–1497.

[29] J.M. Pollock, A.R. Deibler, T.G. West, J.H. Burdette, R.A. Kraft, J.A. Maldjian, Arterial spin-labeled magnetic resonance imaging in hyperperfused seizure focus: a case report, J. Comput. Assist. Tomogr. 32 (2) (2008) 291–292.

[30] K.K. Oguz, X. Golay, F.B. Pizzini, C.A. Freer, N. Winrow, R. Ichord, P.C. van Zijl, E.R. Melhem, Sickle cell disease: continuous arterial spin-labeling perfusion MR imaging in children, Radiology 227 (2) (2003) 567–574.

[31] G.E. Chalouhi, M. Alison, B. Deloison, C.A. Cuenod, G. Autret, N. Siauve, L. Salomon, J Assessment of Feto-Placental Oxygenation in an Intra-uterine Growth Restriction Rat Model, Using Blood Oxygen Level-dependent (BOLD) MRI at 4.7 Tesla, Radiology under Review, (2013).

[32] M. Alison, G.E. Chalouhi, G. Autret, D. Balvay, R. Thiam, L.J. Salomon, C.A. Cuenod, O. Clement, N. Siauve, Use of intravoxel incoherent motion MR imaging to assess placental perfusion in a murine model of placental insufficiency, Invest. Radiol. 48 (1) (2013) 17–23.

[33] J.S. Wigglesworth, Experimental growth retardation in the foetal rat, J. Pathol. Bacteriol. 88 (1964) 1–13.

[34] F. Kober, I. Iltis, M. Izquierdo, M. Desrois, D. Ibarrola, P.J. Cozzone, M. Bernard, High-resolution myocardial perfusion mapping in small animals in vivo by spin-labeling gradient-echo imaging, Magn. Reson. Med. : Offic. J. Soc. Magn. Reson. Med./Soc. Magn. Reson. Med. 51 (1) (2004) 62–67.

[35] G. Duhamel, V. Callot, P.J. Cozzone, F. Kober, Spinal cord blood flow measurement by arterial spin labeling, Magn. Reson. Med.: Offic. J. Soc. Magn. Reson. Med./Soc. Magn. Reson. Med. 59 (4) (2008) 846–854.

[36] V. Belle, E. Kahler, C. Waller, E. Rommel, S. Voll, K.H. Hiller, W.R. Bauer, A. Haase, In vivo quantitative mapping of cardiac perfusion in rats using a noninvasive MR spin-labeling method, J. Magn. Reson. Imag. 8 (6) (1998) 1240–1245.

[37] S.G. Kim, N.V. Tsekos, Perfusion imaging by a flow-sensitive alternating inversion recovery (FAIR) technique: application to functional brain imaging, Magn. Reson. Med. : Offic. J. Soc. Magn. Reson. Med./Soc. Magn. Reson. Med. 37 (3) (1997) 425–435.

[38] F. Taillieu, L.J. Salomon, N. Siauve, O. Clement, N. Faye, D. Balvay, C. Vayssettes, G. Frija, Y. Ville, C.A. Cuenod, Placental perfusion and permeability: simultaneous assessment with dual-echo contrast-enhanced MR imaging in mice, Radiology 241 (3) (2006) 737–745.

[39] U.D.N.M.V.C.R.N.F.N.I.d.M.P.C.M.A.M. BrasilI, Methodology to study the volume and absolute placental density in human placenta at term, Rev. Bras. Ginecol. Obstet. 24 (10) (2002).

[40] R. Gagnon, Placental insufficiency and its consequences, Eur. J. Obstet. Gynecol. Reprod. Biol. 110 (Suppl 1) (2003) S99–S107.

[41] G. Pardi, A.M. Marconi, I. Cetin, Placental-fetal interrelationship in IUGR fetuses-a review, Placenta 23 (Suppl A) (2002) S136–S141.

[42] M. Gilbert, A. Leturque, Fetal weight and its relationship to placental blood flow and placental weight in experimental intrauterine growth retardation in the rat, J. Dev. Physiol. 4 (4) (1982) 237–246.

[43] L. Bricker, J.P. Neilson, Routine Doppler ultrasound in pregnancy, Cochrane Database Syst. Rev. 2 (2000) CD001450.

[44] L. Bricker, J.P. Neilson, WITHDRAWN: routine Doppler ultrasound in pregnancy, Cochrane Database Syst. Rev. 2 (2007) CD001450.

[45] C.A. Meads, J.S. Cnossen, S. Meher, A. Juarez-Garcia, G. ter Riet, L. Duley, T.E. Roberts, B.W. Mol, J.A. van der Post, M.M. Leeflang, P.M. Barton, C.J. Hyde, J.K. Gupta, K.S. Khan, Methods of prediction and prevention of pre-eclampsia: systematic reviews of accuracy and effectiveness literature with economic modelling, Health Technol. Assess. 12 (6) (2008) 1–270 iii-iv.

[46] K.K. Kwong, D.A. Chesler, R.M. Weisskoff, K.M. Donahue, T.L. Davis, L. Ostergaard, T.A. Campbell, B.R. Rosen, MR perfusion studies with T1-weighted echo planar imaging, Magn. Reson. Med. : Offic. J. Soc. Magn. Reson. Med./Soc. Magn. Reson. Med. 34 (6) (1995) 878–887.

[47] S.G. Kim, Quantification of relative cerebral blood flow change by flow-sensitive alternating inversion recovery (FAIR) technique: application to functional mapping, Magn. Reson. Med. : Offic. J. Soc. Magn. Reson. Med./Soc. Magn. Reson. Med. 34 (3) (1995) 293–301.

[48] C. Schwarzbauer, S.P. Morrissey, A. Haase, Quantitative magnetic resonance imaging of perfusion using magnetic labeling of water proton spins within the detection slice, Magn. Reson. Med. : Offic. J. Soc. Magn. Reson. Med./Soc. Magn. Reson. Med. 35 (4) (1996) 540–546.